Biomimetic Intelligence and Robotics 3 (2023) 100116

Contents lists available at ScienceDirect

Biomimetic Intelligence and Robotics

journal homepage: www.elsevier.com/locate/birob

Research Article

Bioinspired backstepping sliding mode control and adaptive sliding innovation filter of quadrotor unmanned aerial vehicles

Zhe Xu [a], Tao Yan [a], Simon X. Yang [a,*], S. Andrew Gadsden [b]

[a] School of Engineering, University of Guelph, Guelph N1G 2V7, Canada
[b] Department of Mechanical Engineering, McMaster University, Hamilton L8S 4L8, Canada

ARTICLE INFO

Article history:
Received 4 May 2023
Revised 21 June 2023
Accepted 20 July 2023
Available online 26 July 2023

Keywords:
Trajectory tracking
Backstepping sliding mode
Sliding innovation filter
Unmanned aerial vehicle

ABSTRACT

Quadrotor unmanned aerial vehicles have become the most commonly used flying robots with wide applications in recent years. This paper presents a bioinspired control strategy by integrating the backstepping sliding mode control technique and a bioinspired neural dynamics model. The effects of both disturbances and system and measurement noises on the quadrotor unmanned aerial vehicle control performance have been addressed in this paper. The proposed control strategy is robust against disturbances with guaranteed stability proven by the Lyapunov stability theory. In addition, the proposed control strategy is capable of providing smooth control inputs under noises. Considering the modeling uncertainties, the adaptive sliding innovation filter is integrated with the proposed control to provide accurate state estimates to improve tracking effectiveness. Finally, the simulation results demonstrate that the proposed control strategy provides satisfactory tracking performance for a quadrotor unmanned vehicle operating under disturbances and noises.

1. Introduction

There has been an increasing trend for the research on unmanned aerial vehicles (UAVs) over the past decade due to its extensive applications in many areas [1–3], such as military reconnaissance, disaster monitoring, and traffic recognition. The evolving technology in real-time computing, processing power, and remote control capabilities has enabled the development of modern UAVs, which usually operate in high-risk and complicated environments that pose potential hazards to human beings. Therefore, considering safety, cost effectiveness, and task efficiency, UAVs have become one of the most attractive options.

The quadrotor is the most commonly used UAV platform and has been drawing most of the attention in UAV research. The major advantages of the quadrotor UAV are that it has excellent maneuverability, vertical landing and take-off capability, and hovering capability, and it can operate in indoor or outdoor environments, giving great flexibility to complete the required tasks. Although the quadrotor has these advantages, designing for efficiency and effectiveness in the controller has become quite challenging due to its high non-linearity, underactuation, coupling, and operating conditions, such as disturbances and noises.

There are many interesting research topics in robotics [4,5], and the control design has always been an interesting topic [6,7] and extensive research on robust control of the quadrotor UAV regarding the disturbances has been conducted. The backstepping sliding mode control is a commonly used method that is robust to disturbances [8–10]. There are various adaptive sliding mode control methods are also developed to address the uncertainties in the dynamics of quadrotor UAV [11–13]. Although these approaches are capable of reducing the effects that are caused by disturbances, when there are system and measurement noises, these sliding mode based approaches still have control input chattering. The model predictive control is another approach that can deal with disturbances [14,15], however, this method often only considers the kinematics of the UAV and does not consider the dynamic model. Additionally, this method is computationally complex and requires online optimization, which would be difficult to implement on a real quadrotor UAV for real-world applications. The machine learning technique such as neural networks [16,17] and reinforcement learning approaches [18–20] are popular methods and robust to disturbances; however the neural networks requires training and could be computationally expensive. As for reinforcement learning, the inadequate design of reward function could result in undesirable behavior in real world applications, and its trial and error based learning process could be problematic in the data collection, especially for platforms like quadrotor UAVs. The other approach that addresses disturbances is observer based control [21–23]; however, this method often makes the assumption that the disturbances are continuous and the derivative of the disturbances is bounded as well. In addition, this method relies on the accuracy of the state

* Corresponding author.
E-mail address: syang@uoguelph.ca (S.X. Yang).

https://doi.org/10.1016/j.birob.2023.100116

feedback and high gain, which would provide rapidly changing estimates that is unreliable. The above methods have made great contributions to robot operates under disturbances; however, it is observed that these methods lack consideration of noise. It is noted that the backstepping sliding mode technique has been widely adopted for the control of quadrotor UAVs, due to its excellent robustness to disturbances and it is a straightforward method with guaranteed stability proven by the Lyapunov stability theory [24–26].

Besides, to address the noises, there are several studies that considered the Gaussian distributed noises [27,28], it is noted that the linear quadratic Gaussian method is capable of providing smooth control inputs for the quadrotor operating under noises [27]. However, the quadrotor UAV is a highly nonlinear system, and this method requires linearization, thus only guaranteeing local stability. For the linear quadratic Gaussian method, although it can address the noises that is Gaussian distributed when the disturbances do not satisfy this distribution, the control performance and its stability cannot be guaranteed. In addition, these methods often integrate with the Kalman filter, which provides optimal results with no modeling errors or uncertainties, and when there are modeling errors, the accuracy of the state estimates may have a huge impact on the accuracy of the tracking control.

Based on the reviewed results above, the main objective of this paper is to address the limitations of many existing works, which mostly focus on either noises or disturbances. Thus, it is necessary to develop an efficient and robust tracking control strategy for a quadrotor UAV operating under these two effects. In addition, accurately obtaining the system matrix is challenging due to the presence of disturbances, the Kalman filter may provide inaccurate state estimates and diverge the tracking error. Thus, to enhance the accuracy during the estimation process, it is critical to incorporate a robust filtering strategy that can handle these uncertainties and improves the operational practicability of quadrotor UAVs. Overall, this paper directly tackles these aforementioned issues and develops a backstepping sliding mode controller aided with bioinspired neural dynamics that is suitable for quadrotor UAVs. The main contribution of this paper is listed as follows:

(1) The bioinspired backstepping sliding mode controller has been developed to address the tracking control problem of the quadrotor UAV that operates under disturbances and noises.

(2) Compared to the conventional approach, the proposed method is not only robust against disturbances but also offers smooth control inputs under noises by utilizing the characteristics of the bioinspired neural dynamics in the control. The proposed bioinspired control method is proved to be stable using Lyapunov stability theory.

(3) Considering the noises, the proposed control is integrated with the adaptive sliding innovation filter (ASIF) to provide accurate state estimates and robust to modeling error.

The rest of the paper is organized as follows: Section 2 provides the model of the quadrotor UAV. Then, Section 3 demonstrates the design procedures of the bioinspired backstepping sliding mode control that is integrated with the ASIF. After that, Section 4 provides various simulation results that show the advantages of the proposed control method. Finally, Section 5 gives a conclusion and possible future works on the proposed method.

2. Modeling of quadrotor UAV

The quadrotor has six degrees of freedom with four rotor inputs; therefore, it is an underactuated system. The six degrees of freedom include its translational motion x, y and z. and rotational motion ϕ, θ and ψ. Fig. 1 shows the schematic of a quadrotor

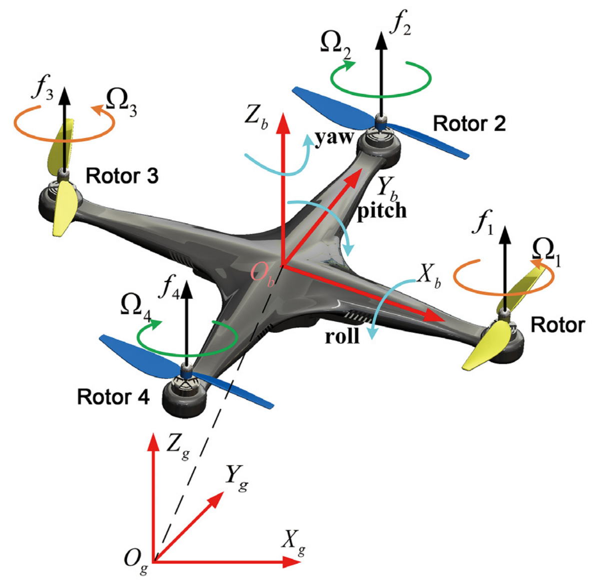

Fig. 1. Schematic diagram of a quadrotor UAV.

UAV, in which four rotors generate propeller forces that drive the quadrotor UAV to move and each rotor is separately controlled by a motor. In addition, to counter the torque effects of a single rotor when spinning, the Rotors 1 and 3 spinning direction is opposite to Rotors 2 and 4. The two coordinates systems, body fixed frame and inertial frame are represented by $O_bX_bY_bZ_b$ and $O_gX_gY_gZ_g$, respectively. The vertical translational motion of the quadrotor UAV can be achieved by identically changing the rotational speed of each rotor to provide less propeller force. As for the three rotational motions, the roll motion p is reached by changing the rotational speed of Rotors 2 and 4. Similarly, by changing the rotational speed of Rotors 1 and 3, the quadrotor UAV will perform a pitch q motion. Lastly, since two pairs of rotors rotate opposite to each other, the yaw r motion is performed from the torque differences between the two pairs of rotors.

Although the quadrotor UAV is a complicated system, the entire system can be divided into translational and rotational subsystems that strongly couple with each other. To develop the model of the quadrotor, the following assumption needs to hold.

Assumption 1. It is assumed that the quadrotor UAV is a rigid body and structurally symmetric.

Furthermore, the pitch and roll angle are bounded between $(-\frac{\pi}{2}, \frac{\pi}{2})$ and the yaw angle is bounded to $(-\pi, \pi)$. Denote $\eta = \begin{bmatrix} \eta_x & \eta_y & \eta_z \end{bmatrix}^T$ and $\xi = \begin{bmatrix} \xi_\phi & \xi_\theta & \xi_\psi \end{bmatrix}^T$ are respectively the quadrotor position and rotational angles. In addition, the rotation matrix from the body fixed frame to the inertial frame is given by

$$J_r = \begin{bmatrix} C_\psi C_\theta & S_\phi C_\psi S_\theta - C_\phi S_\psi & C_\phi C_\psi S_\theta + S_\phi S_\psi \\ S_\psi C_\theta & S_\phi S_\psi S_\theta + C_\phi C_\psi & C_\phi S_\psi S_\theta - S_\phi C_\psi \\ -S_\theta & S_\phi C_\theta & C_\phi C_\theta \end{bmatrix} \tag{1}$$

where C and S represent cosine and sine functions, respectively; ϕ, ψ and θ are respectively the roll, yaw, and pitch angle of the UAV in the inertial frame; J_r is an orthogonal matrix, which means that $\det(J_r) = 1$ if J_r is nonsingular. In addition, J_r also meets the condition that $\dot{J}_r = J_rQ(\omega)$, where $\omega = [p, q, r]^{\mathrm{T}}$ is the angular velocity with respect to the body-fixed frame for roll, pitch, and yaw motions. Matrix $Q(\omega)$ is a skew symmetric matrix, which is defined as

$$Q(\omega)=\begin{bmatrix} 0 & -r & q \\ r & 0 & -p \\ -q & p & 0 \end{bmatrix} \tag{2}$$

The relation between the rotational speed in the inertial frame and body fixed frame is given by

$$\dot{\xi}=R_r\omega \tag{3}$$

where R_r is provided as

$$R_r=\begin{bmatrix} 1 & 0 & -S_\phi \\ 0 & C_\phi & S_\phi C_\theta \\ 0 & -S_\phi & C_\phi C_\theta \end{bmatrix} \tag{4}$$

Then, the translational and rotational dynamics of the quadrotor UAV are given based on Newton–Euler formula as [9,29]

$$m\ddot{\eta}=J_rF+G_g+F_D \tag{5}$$

$$I\dot{\omega}=-\omega\times I\omega+G_f+\tau_M+\tau_c \tag{6}$$

where m is the mass of the quadrotor UAV, I is the rotary inertia in the body fixed frame, which is given as $I=\mathrm{diag}(I_{xx},I_{yy},I_{zz})$ and I_{xx}, I_{yy}, and I_{zz} are the inertia with respect to X_b, Y_b, and Z_b; F is the total thrust; G_g is the gravitational force; τ_M is the gyroscope effects; F_D is forced from the gyroscope effects; τ_c is the torque generated by four rotors. In addition, the thrust force generated from each propeller is assumed to be proportional to the square of the propeller speed. Therefore F is defined as

$$F=\begin{bmatrix} 0 & 0 & \sum_{i=1}^{4} f_i \end{bmatrix}^T=\begin{bmatrix} 0 & 0 & k_d\sum_{i=1}^{4}\Omega_i^2 \end{bmatrix}^T \tag{7}$$

where k_d is called the thrust factor, f_i is the thrust generated by each rotor, and Ω_i is the rotary speed of each rotor. The forces of the gyroscope effects F_D is written as

$$F_D=\begin{bmatrix} -c_{dx} & 0 & 0 \\ 0 & -c_{dy} & 0 \\ 0 & 0 & -c_{dz} \end{bmatrix}\begin{bmatrix} \dot{x} \\ \dot{y} \\ \dot{z} \end{bmatrix} \tag{8}$$

where c_{dx}, c_{dy}, and c_{dz} are, respectively, the air drag coefficients. The gravitational force G_g of the quadrotor UAV is given as

$$G_g=\begin{bmatrix} 0 & 0 & -mg \end{bmatrix}^T \tag{9}$$

where g is the gravitational constant, and the aerodynamic friction torque G_f is given as

$$G_f=\begin{bmatrix} k_{dx} & 0 & 0 \\ 0 & k_{dy} & 0 \\ 0 & 0 & k_{dz} \end{bmatrix}\|\omega\|^2 \tag{10}$$

where k_{dx}, k_{dy}, and k_{dz} are aerodynamic friction factors and the gyroscope effects τ_M is given as

$$\tau_M=-\sum_{i=1}^{4} I_r\omega^T\begin{bmatrix} 0 \\ 0 \\ (-1)^{i+1}\Omega_i \end{bmatrix} \tag{11}$$

where I_r is the rotor inertia, the control torque that is generated by four rotors in the body fixed frame is defined as

$$\tau_c=\begin{bmatrix} l(f_1-f_3) \\ l(f_2-f_4) \\ k_p(\Omega_1^2+\Omega_3^2-\Omega_2^2-\Omega_4^2) \end{bmatrix} \tag{12}$$

where k_p is the drag factors, and l is the distance between the center of the mass to the rotor. By considering the fact that rotational angles are within a small neighborhood of their equilibrium points, the resulting perturbed dynamics of the quadrotor UAV is computed to be [9,29]

$$\begin{cases} \ddot{\eta}_x=-\dfrac{1}{m}c_{dx}\dot{x}+\dfrac{1}{m}\left(C_\phi C_\psi S_\theta+S_\phi S_\psi\right)U_1+d_x \\ \ddot{\eta}_y=-\dfrac{1}{m}c_{dy}\dot{y}+\dfrac{1}{m}\left(C_\phi S_\psi S_\theta-S_\phi C_\psi\right)U_1+d_y \\ \ddot{\eta}_z=-\dfrac{1}{m}c_{dz}\dot{z}-g+\dfrac{1}{m}\left(C_\phi C_\theta\right)U_1+d_z \end{cases} \tag{13}$$

$$\begin{cases} \ddot{\xi}_\phi=(\dfrac{I_{yy}-I_{zz}}{I_{xx}})\dot{\theta}\dot{\psi}-\dfrac{I_r\bar{\Omega}}{I_{xx}}\dot{\theta}-\dfrac{k_{dx}}{I_{xx}}\dot{\phi}^2+\dfrac{l}{I_{xx}}U_2+d_\phi \\ \ddot{\xi}_\theta=(\dfrac{I_{zz}-I_{xx}}{I_{yy}})\dot{\phi}\dot{\psi}-\dfrac{I_r\bar{\Omega}}{I_{yy}}\dot{\phi}-\dfrac{k_{dy}}{I_{yy}}\dot{\theta}^2+\dfrac{l}{I_{yy}}U_3+d_\theta \\ \ddot{\xi}_\psi=(\dfrac{I_{xx}-I_{yy}}{I_{zz}})\dot{\phi}\dot{\theta}--\dfrac{k_{dz}}{I_{zz}}\dot{\psi}^2+\dfrac{1}{I_{zz}}U_4+d_\psi \end{cases} \tag{14}$$

where $\bar{\Omega}=\Omega_1-\Omega_2+\Omega_3-\Omega_4$ which is shown in Fig. 1; d_x to d_ψ are the disturbances. The input $U=\begin{bmatrix} U_1 & U_2 & U_3 & U_4 \end{bmatrix}^T$ is defined as

$$\begin{bmatrix} U_1 \\ U_2 \\ U_3 \\ U_4 \end{bmatrix}=\begin{bmatrix} k_d & k_d & k_d & k_d \\ 0 & k_d & 0 & -k_d \\ -k_d & 0 & k_d & 0 \\ k_p & -k_p & k_p & -k_p \end{bmatrix}\begin{bmatrix} \Omega_1^2 \\ \Omega_2^2 \\ \Omega_3^2 \\ \Omega_4^2 \end{bmatrix} \tag{15}$$

Assumption 2. The disturbances $d_1=\begin{bmatrix} d_x & d_y & d_z \end{bmatrix}^T$ and $d_2=\begin{bmatrix} d_\phi & d_\theta & d_\psi \end{bmatrix}^T$ are unknown but bounded, such that $|d_i|\le\gamma_i$ for $i\in\{x,y,z\}$ and $|d_j|\le\gamma_j$ for $j\in\{\phi,\theta,\psi\}$.

3. Design of bioinspired neural dynamic based control

To address the tracking control problem for a quadrotor UAV operating under noises and disturbances, this section designs a bioinspired backstepping sliding mode control that is integrated with the adaptive sliding innovation filter. Based on the characteristics of the quadrotor UAV, the UAV contains two parts, which are transitional dynamics and rotational dynamics. Then, the goal is to design the controller that stabilizes the quadrotor systems while remaining its robustness against disturbances with smooth control inputs. The accuracy of the state estimates is considered since the quadrotor UAV could operate in noisy environments. In addition, the proposed control strategy aims to provide smooth control inputs when system and measurement noises occur. Fig. 2 is the schematic of the bioinspired backstepping control strategy for the quadrotor UAV, in which four control inputs need to stabilize the quadrotor system that contains six degrees of freedom.

3.1. Bioinspired neural dynamics

The following control design is heavily based on a membrane model that was first proposed by Hodgkin and Huxley [30] to illustrate a patch of membrane using electrical elements. This model was later used to develop the bioinspired neural dynamic model by Grossberg [31]. Then, Yang and Meng first applied this model to robotic research [32], which was later extended to many works and various areas [33–36]. This neural dynamics model is given as

$$\dot{V}_{s,i}=-A_iV_{s,i}+(B_i-V_{s,i})f(e_i)-(D_i+V_{s,i})g(e_i) \tag{16}$$

where e_i is the error between the desired state and the estimated state of the quadrotor, $f(e_i)$ and $g(e_i)$ are respectively set to be $f(e_i)=\max\{e_i,0\}$ and $g(e_i)=\max\{-e_i,0\}$. From the unique

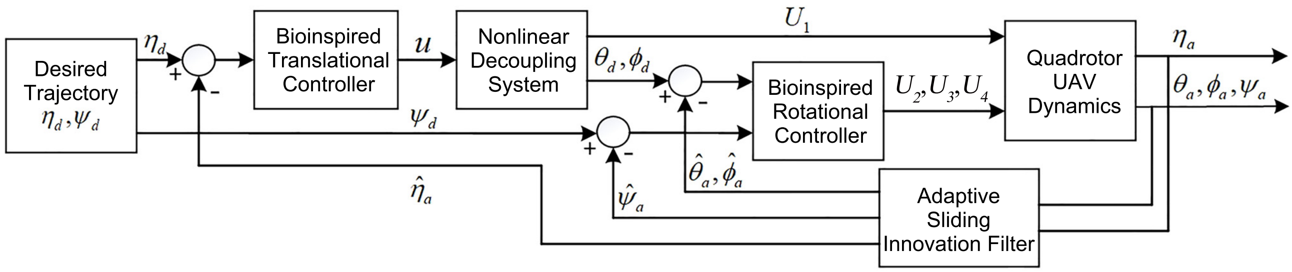

Fig. 2. Block diagram of a UAV based on the bioinspired control strategy and sliding innovation filter.

characteristics of the shunting model, the output $V_{s,i}$ is bounded between the interval $[-D_i, B_i]$ with a smooth output. In order to extend (16) from scalar form to a higher dimension for the control of quadrotor UAV, (16) is rewritten as

$$\dot{V}_s = -\Lambda V_s + G \tag{17}$$

where $V_s = \begin{bmatrix} V_{s1} & \dots & V_{sn} \end{bmatrix}^T \in R^n$, Λ and G are respectively defined as

$$\begin{aligned} &\Lambda = A + E \\ &A = \mathrm{diag}\begin{pmatrix} A_1 & \dots & A_n \end{pmatrix} \\ &E = \mathrm{diag}\begin{pmatrix} |e_1| & \dots & |e_n| \end{pmatrix} \\ &G = \begin{cases} B_i e_i & \text{if} \quad e_i \geq 0 \quad \text{for} \quad i \in \{1, \dots, n\} \\ D_i e_i & \text{if} \quad e_i < 0 \quad \text{for} \quad i \in \{1, \dots, n\} \end{cases} \end{aligned} \tag{18}$$

where B and D are defined as $B = \mathrm{diag}(B_1, \dots, B_n)$ and $D = \mathrm{diag}(D_1, \dots, D_n)$, respectively.

Remark 1. In (16), regarding e_i as the input, if e_i is bounded, $V_{s,i}$ is input to state stable, if $e_i \to 0$ as $t \to \infty$, then, $V_{s,i} \to 0$. In addition, the output of the shunting model is dynamic to environmental changes, this implies that $V_{s,i}$ has more consistent behavior under noises. Furthermore, V_s is strictly bounded within $(-D_i, B_i)$. Thus, the following controller design utilizes the advantages of this bioinspired neural dynamics.

3.2. Translational control design

Considering the disturbances, the proposed bioinspired control design aims to stabilize the translational dynamics using a recursive design based on the Lyapunov approach. In addition, under system and measurement noises, the proposed controller is capable of providing smooth control input that requires less control effort to control the UAV compared with conventional design, which is critical in real-world applications.

First, based on the backstepping control design approach, the position error is defined as

$$e_p = \eta_d - \eta_a \tag{19}$$

where $\eta_d = \begin{bmatrix} \eta_{d,x} & \eta_{d,y} & \eta_{d,z} \end{bmatrix}^T \in R^3$ and $\eta_a = \begin{bmatrix} \eta_{a,x} & \eta_{a,y} & \eta_{a,z} \end{bmatrix}^T \in R^3$ are respectively the desired position and the actual position of the quadrotor UAV. Then, the Lyapunov candidate function is proposed as

$$V_1 = \frac{1}{2} e_p^T e_p + \frac{1}{2} V_{s1}^T K_1 B_1^{-1} V_{s1} \tag{20}$$

where $K_1 = \mathrm{diag}\left(K_{1,x}, K_{1,y}, K_{1,z}\right)$ and $B_1 = \mathrm{diag}(B_{1,x}, B_{1,y}, B_{1,z})$ are the positive definite diagonal design matrices. Then, by assuming $B_1 = D_1$ and treating $A_1 = \mathrm{diag}\left(A_{1,x}, A_{1,y}, A_{1,z}\right)$ as a positive definite diagonal design matrix, regarding α_1 as the virtual control input, the time derivative of V_1 is written as

$$\begin{aligned} \dot{V}_1 &= e_p^T \dot{e}_p + V_{s1}^T K_1 B_1^{-1} \dot{V}_{s1} \\ &= e_p^T \left(\dot{\eta}_d - \dot{\eta}_a\right) - V_{s1}^T K_1 B_1^{-1} \Lambda_1 V_{s1} + V_{s1}^T K_1 B_1^{-1} B_1 e_p \\ &= e_p^T \left(\dot{\eta}_d - \alpha_1\right) - V_{s1}^T K_1 B_1^{-1} \Lambda_1 V_{s1} + V_{s1}^T K_1 e_p \end{aligned} \tag{21}$$

Then, in order to stabilize the virtual system, it is designed as

$$\alpha_1 = \dot{\eta}_d + K_1 V_{s1} \tag{22}$$

By substituting (22) into (21), $\dot{V}_1$ becomes

$$\dot{V}_1 = -V_{s1}^T K_1 B_1^{-1} \Lambda_1 V_{s1} \leq 0 \tag{23}$$

Based on (23), it can be found that $V_1 \to 0$ as $t \to \infty$, from which it implies $V_{s1,i} \to 0$ as $t \to \infty$ $i \in \{x, y, z\}$. Then, based on the shunting equation defined in (17), if $V_{s1,i} \to 0$, then $e_{p,i} \to 0$ as well. Thus, the equilibrium point $e_{p,i} = 0$ is asymptotically stable. After that, the second state tracking error is defined as

$$e_\upsilon = \alpha_1 - \dot{\eta}_a \tag{24}$$

The Lyapunov candidate function is proposed as

$$V_2 = V_1 + \frac{1}{2} e_\upsilon^T e_\upsilon + \frac{1}{2} V_{s2}^T K_2 B_2^{-1} V_{s2} \tag{25}$$

where $K_2 = \mathrm{diag}\left(K_{2,x}, K_{2,y}, K_{2,z}\right)$, $A_2 = \mathrm{diag}(A_{2,x}, A_{2,y}, A_{2,z})$, and $B_2 = \mathrm{diag}\left(B_{2,x}, B_{2,y}, B_{2,z}\right)$ are positive definite diagonal matrices. Assuming $B_2 = D_2$, then, based on (22), the time derivative of V_2 is calculated as

$$\begin{aligned} \dot{V}_2 =& e_p^T(e_\upsilon - K_1 V_{s1}) + e_\upsilon^T \dot{e}_\upsilon + \sum_{i=1}^{2} V_{si}^T K_i B_i^{-1} \dot{V}_{si} \\ =& -e_p^T K_1 V_{s1} + e_\upsilon^T(\ddot{\eta}_d + K_1 \dot{V}_{s1} - \ddot{\eta}_a + e_p) + V_{s1}^T K_1 e_p \\ &+ V_{s2}^T K_2 e_\upsilon - \sum_{i=1}^{2} V_{si}^T K_i B_i^{-1} \Lambda_i V_{si} \\ =& e_\upsilon^T(\ddot{\eta}_d + K_1 \dot{V}_{s1} - f(\eta_a) + e_p + d_1 - U) + V_{s2}^T K_2 e_\upsilon \\ &- \sum_{i=1}^{2} (V_{si}^T K_i B_i^{-1} A_i V_{si} - V_{si}^T K_i B_i^{-1} E_i V_{si}) \end{aligned} \tag{26}$$

where $f(\eta_a) \in R^3$ is the nonlinear function in (13) excludes the control input and disturbances and the control law that stabilize the position of the quadrotor UAV is defined as

$$U = \begin{bmatrix} U_x & U_y & U_z \end{bmatrix}^T = \ddot{\eta}_{d,i} - f(\eta_a) + K_1 \dot{V}_{s1} + e_p + K_2 V_{s2} \tag{27}$$

Theorem 1. *Given the disturbed dynamic model described in (13) along with Assumption 2, by substituting the proposed control law (27) into (13), the translational dynamics is input to state stable.*

Proof. Define $E_2^l = \begin{bmatrix} |e_{\upsilon,x}| & |e_{\upsilon,y}| & |e_{\upsilon,z}| \end{bmatrix}$ and $L_1 = \begin{bmatrix} |d_x| & |d_y| & |d_z| \end{bmatrix}^T$, by substituting (22) and (27) into (26), $\dot{V}_2$ is rewritten as

$$\begin{aligned} \dot{V}_2 =& -\sum_{i=1}^{2} (V_{si}^T K_i B_i^{-1} A_i V_{si} + V_{s1}^T K_i B_i^{-1} E_i V_{si}) + {e_\upsilon}^T d_1 \\ \leq& - V_{s2}^T K_2 B_2^{-1} A_2 V_{s2} - V_{s2}^T K_2 B_2^{-1} E_2 V_{s2} + {e_\upsilon}^T d_1 \\ \leq& - V_{s2}^T K_2 B_2^{-1} E_2 V_{s2} + E_2^l L_1 \end{aligned} \tag{28}$$

It follows from the last line of (28), by expanding this equation, it is calculated that

$$\dot{V}_2 \leq \sum_{i\in\{x,y,z\}} |e_i|(-\frac{K_{2,i}V_{s2,i}^2}{B_{2,i}} + |d_i|) \tag{29}$$

It is obvious whenever $\frac{K_{2,i}V_{s2,i}^2}{B_{2,i}} \geq |d_i|$, $\dot{V}_2 \leq 0$. Consequently, e_p, e_v are bounded. It is necessary to note that $V_{s2,i}$ is bounded between the finite interval $(-D_{2,i}, B_{2,i})$, since it is set that $D_{2,i} = B_{2,i}$. To ensure the stability of the system, the parameters $K_{2,i}$ and $B_{2,i}$ have to satisfy $K_{2,i}B_{2,i} \geq |\gamma_i|$. This proof has completed. ■

Remark 2. Compared to the conventional backstepping sliding mode control design, all the error terms are replaced by shunting models, which is robust against disturbances. In addition, considering the system and measurement noises, the shunting model acts as a low-pass filter that is capable of providing smooth control input. Finally, the stability of the control design has been proved.

From the translational dynamics defined in (13), the control inputs from (27) in translational dynamics are also defined as

$$\begin{cases} U_x = \dfrac{1}{m}\left(C_\phi C_\psi S_\theta + S_\phi S_\psi\right) U_1 \\ U_y = \dfrac{1}{m}\left(C_\phi S_\psi S_\theta - S_\phi C_\psi\right) U_1 \\ U_z = \dfrac{1}{m}\left(C_\phi C_\theta\right) U_1 - g \end{cases} \tag{30}$$

Then, based on (30), the desired angles are given as

$$\begin{cases} \phi_d = \arctan\left(\dfrac{C_{\theta_d}\left(U_x S_{\psi_d} - U_y C_{\psi_d}\right)}{U_z + g}\right) \\ \theta_d = \arctan\left(\dfrac{U_x C_{\psi_d} + U_y S_{\psi_d}}{U_z + g}\right) \end{cases} \tag{31}$$

and the total thrust generated from four propellers are calculated as

$$U_1 = m\sqrt{U_x^2 + U_y^2 + (U_z + g)^2} \tag{32}$$

The bioinspired backstepping sliding mode positional control for a quadrotor UAV is proposed. The bioinspired neural dynamics that is integrated with the conventional design provides smooth control input under the system and measurement noises due to the filtering capability from the bioinspired neural dynamics. In addition, the proposed control offers extra robustness to disturbances and the control input is bounded by the shunting model as well.

3.3. Rotational control design

The proposed bioinspired backstepping positional control is capable of tracking its desired position, however, the controller has difficulties in realizing its rotation angle. Thus, this section designs a backstepping sliding mode controller for the rotational dynamics to ensure the stability of the tracking angle with smooth control input under the noises and robustness to disturbances as well.

Define the angular tracking error as

$$e_\omega = \xi_d - \xi_a \tag{33}$$

where $\xi_d = [\xi_{d,\phi}, \xi_{d,\theta}, \xi_{d,\psi}]^T$ and $\xi_a = [\xi_{a,\phi}, \xi_{a,\theta}, \xi_{a,\psi}]^T$ are respectively the desired and actual rotational angles. Then, the Lyapunov candidate function is proposed as

$$V_3 = \frac{1}{2}e_\omega^T e_\omega + \frac{1}{2}V_{s3}^T K_3 B_3^{-1} V_{s3} \tag{34}$$

where $K_3 = \mathrm{diag}(K_{3,\phi}, K_{3,\theta}, K_{3,\psi})$ and $B_3 = \mathrm{diag}(B_{3,\phi}, B_{3,\theta}, B_{3,\psi})$ are the positive definite diagonal matrices, $V_{s3} = \mathrm{diag}(V_{s3,\phi}, V_{s3,\theta}, V_{s3,\psi})$ is the output of the shunting model with respect to the input e_ω. Considering α_2 as virtual control input, by setting $B_3 = D_3$; then, $\dot{V}_3$ is calculated as

$$\begin{aligned} \dot{V}_3 =& e_\omega^T \dot{e}_\omega + V_{s3}^T K_3 B_3^{-1} \dot{V}_{s3} \\ =& e_\omega^T\left(\dot{\xi}_d - \dot{\xi}_a\right) - V_{s3}^T K_3 B_3^{-1} \Lambda_3 V_{s3} + V_{s3}^T K_3 B_3^{-1} B_3 e_\omega \\ =& e_\omega^T\left(\dot{\xi}_d - \alpha_2\right) - V_{s3}^T K_3 B_3^{-1} \Lambda_3 V_{s3} + V_{s3}^T K_3 e_\omega \end{aligned} \tag{35}$$

In order to stabilize the rotational subsystem, the virtual controller α_k is designed as

$$\alpha_2 = \dot{\xi}_d + K_3 V_{s3} \tag{36}$$

By substituting (36) into (35), $\dot{V}_3$ is rewritten as

$$\dot{V}_3 = -V_{s3}^T K_3 B_3^{-1} \Lambda_3 V_{s3} \tag{37}$$

Thus, $\dot{V}_3 \to 0$ as $t \to \infty$, which implies $V_{s3,i} \to 0$ for $i \in \{\phi, \theta, \psi\}$. Based on the input output properties of the shunting model that is defined in (17), if $V_{s3,i} \to 0$, as $t \to \infty$, $e_{w,i} \to 0$ as well. Therefore, the equilibrium point $e_{w,i} = 0$ is asymptotically stable.

The rotational controller follows by a recursive design, the second state tracking error is firstly defined as

$$e_\mu = \alpha_2 - \dot{\xi}_a \tag{38}$$

Then, the Lyapunov candidate function is proposed as

$$V_4 = V_3 + \frac{1}{2}e_\mu^T e_\mu + \frac{1}{2}V_{s4}^T K_4 B_4^{-1} V_{s4} \tag{39}$$

where $K_4 = \mathrm{diag}(K_{4,\phi}, K_{4,\theta}, K_{4,\psi})$ and $B_4 = \mathrm{diag}(B_{4,\phi}, B_{4,\theta}, B_{4,\psi})$ are positive definite diagonal matrices, regarding e_μ as the input, V_{s4} is the output of the shunting model. Setting $B_4 = D_4$, the time derivative of V_4 is calculated as

$$\begin{aligned} \dot{V}_4 =& \dot{V}_3 + e_\mu^T \dot{e}_\mu + V_{s4}^T K_4 B_4^{-1} \dot{V}_{s4} \\ =& -e_\omega^T K_3 V_{s3} + e_\mu^T(\ddot{\xi}_d + K_3\dot{V}_{s3} - \ddot{\xi}_a + e_\omega) + V_{s3}^T K_3 e_\omega \\ &+ V_{s4}^T K_4 e_\mu - \sum_{i=3}^{4} V_{si}^T K_i B_i^{-1} \Lambda_i V_{si} \\ =& e_\mu^T(\ddot{\xi}_d + K_3\dot{V}_{s3} - f(\xi_a) + e_\omega + d_2 + U_\omega) + V_{s4}^T K_4 e_\mu \\ &- \sum_{i=3}^{4}(V_{si}^T K_i B_i^{-1} A_i V_{si} - V_{si}^T K_i B_i^{-1} E_i V_{si}) \end{aligned} \tag{40}$$

where $f(\xi_a)$ is the nonlinear terms in (14) without disturbances and control inputs, the corresponding control law that stabilizes the rotational dynamics of the quadrotor UAV is given as

$$U_\omega = [U_2 \quad U_3 \quad U_4]^T = \ddot{\xi}_d - f(x) + K_3\dot{V}_{s3} + e_\omega + K_4 V_{s4} \tag{41}$$

It is noted that in (41), $\xi_{d,\phi}$ and $\xi_{d,\theta}$ are calculated from (31), which are then taken into second derivative. This second derivative will cause the so-called term explosion and make the control input impractical. Thus, to avoid such issue, $\ddot{\xi}_{d,\psi}$ is kept in the controller, while $\ddot{\xi}_{d,\phi}$ and $\ddot{\xi}_{d,\theta}$ are removed from the controller, and these two terms are treated as disturbances. The new rotational control inputs are designed as

$$\begin{bmatrix} U_2 \\ U_3 \\ U_4 \end{bmatrix} = \begin{bmatrix} -f(\psi_a) + K_{3,\psi}\dot{V}_{s3,\psi} + e_\omega + K_{4,\psi}V_{s4,\psi} \\ -f(\theta_a) + K_{3,\theta}\dot{V}_{s3,\theta} + e_\theta + K_{4,\theta}V_{s4,\theta} \\ \ddot{\varphi}_d - f(\varphi_a) + K_{3,\varphi}\dot{V}_{s3,\varphi} + e_\varphi + K_{4,\varphi}V_{s4,\varphi} \end{bmatrix} \tag{42}$$

Theorem 2. *Given the disturbed dynamic model described in (14) along with Assumption 2, by substituting the proposed control law (41) into (14), the rotational dynamics is input to state stable.*

Proof. Define $E_4^l = [\ |e_{\mu,\phi}|\quad |e_{\mu,\theta}|\quad |e_{\mu,\psi}|\ ]$, $L_2 = [\ |d_\phi|\quad |d_\theta|\quad |d_\psi|\ ]^T$, and $\ddot{\xi}_d^l = [\ |\ddot{\xi}_{d,\phi}|\quad |\ddot{\xi}_{d,\theta}|\quad 0\ ]^T$. By substituting (41) into (40), $\dot{V}_4$ is rewritten as

$$\begin{aligned}\dot{V}_4 =& -\sum_{i=3}^{4}(V_{si}^T K_i B_i^{-1} A_i V_{si} - V_{s1}^T K_i B_i^{-1} E_i V_{si}) \\ &+ e_\mu^T d_2 + \ddot{\xi}_d^l \\ \leq& V_{s4}^T K_4 B_4^{-1} A_4 V_{s4} - V_{s4}^T K_4 B_4^{-1} E_4 V_{s4} + e_\mu^T d_2 + \ddot{\xi}_d^l \\ \leq& -V_{s4}^T K_4 B_4^{-1} E_4 V_{s4} + E_4^l L_2 + \ddot{\xi}_d^l\end{aligned} \tag{43}$$

By expanding the last line (43), it is calculated that

$$\dot{V}_4 \leq \sum_{i\in\{\phi,\theta,\psi\}} |e_i|(-\frac{K_{4,i}V_{s4,i}^2}{B_{4,i}} + |d_i| + \ddot{\xi}_{d,i}^l) \tag{44}$$

Therefore, whenever $\frac{K_{4,i}V_{s4,i}^2}{B_{4,i}} \geq |d_i| + |\ddot{\xi}_{d,i}|$ for $i \in \{\phi, \theta\}$, based on the special characteristic of the shunting mode, $V_{s4,i}$ is bounded between the finite interval $(-D_{4,i}, B_{4,i})$. Thus, the parameters $K_{4,i}$ and $B_{4,i}$ have to ensure $K_{4,i}B_{4,i} \geq |\gamma_i| + |\ddot{\xi}_{d,i}|$. As for $K_{4,\psi}$ and $B_{4,\psi}$, using a similar approach as shown in Theorem 1, it needs to satisfy $K_{4,\psi}V_{s4,\psi} \geq |d_\psi|$. Thus, $\dot{V}_4 \leq 0$ and V_4 are bounded, consequently e_ω and e_μ are bounded. The proof of Theorem 2 is complete. ■

Then, based on (41) and (14), the rotational controller is written as

$$\begin{aligned}U_2 =& \frac{I_{xx}}{l}((\frac{I_{zz}-I_{yy}}{I_{xx}})\dot{\theta}\dot{\psi} + \frac{\bar{\Omega}}{I_{xx}}\dot{\theta} + \frac{k_{dx}}{I_{xx}}\dot{\phi}^2 + K_{3,\phi}\dot{V}_{s3,\phi} \\ &+ e_{\omega,\phi} + K_{4,\phi}V_{s4,\phi})\end{aligned} \tag{45}$$

$$\begin{aligned}U_3 =& \frac{I_{yy}}{l}((\frac{I_{xx}-I_{zz}}{I_{yy}})\dot{\phi}\dot{\psi} + \frac{\bar{\Omega}}{I_{yy}}\dot{\phi} + \frac{k_{dy}}{I_{yy}}\dot{\theta}^2 + K_{3,\theta}\dot{V}_{s3,\theta} \\ &+ e_{\omega,\theta} + K_{4,\theta}V_{s4,\theta})\end{aligned} \tag{46}$$

$$\begin{aligned}U_4 =& \frac{I_{zz}}{1}((\frac{I_{yy}-I_{xx}}{I_{zz}})\dot{\phi}\dot{\theta} + \frac{k_{dz}}{I_{zz}}\dot{\psi}^2 + \ddot{\xi}_{d,\psi} + K_{3,\psi}\dot{V}_{s3,\psi} \\ &+ e_{\omega,\psi} + K_{4,\psi}V_{s4,\psi})\end{aligned} \tag{47}$$

After the controller is designed as shown in (32), (45)–(47), By substituting the control law defined in (34), (45)–(47) into the quadrotor dynamics in (13) and (14), the input u_k that is defined in (49) is found to be

$$u_k = \begin{bmatrix} \dot{\eta}_{a,x,k} \\ \ddot{\eta}_{d,x,k} + K_{1,x,k}\dot{V}_{s1,x,k} + e_{p,x,k} + K_{2,x,k}V_{s2,x,k} \\ \dots \\ \ddot{\xi}_{d,\psi,k} + K_{3,\psi,k}\dot{V}_{s4\psi,k} + e_{\omega,\psi,k} + K_{4\psi,k}V_{s4,\psi,k} \end{bmatrix} \tag{48}$$

Remark 3. In the conventional design, the $\ddot{\phi}_d, \ddot{\theta}_d$ are calculated by the translational controller, which is then taken into the second derivative. This causes the explosion of control input in the rotational dynamics. Due to the difficulty of computing these second derivatives, these terms are removed in the controller design and regarded as disturbances with proven stability.

Remark 4. The output of the shunting model is bounded between $(-D_{4,i}, B_{4,i})$, thus $K_{4,i}V_{s4,i}$ is ultimately bounded; therefore, it can reduce the input saturation issue compared to conventional methods. In addition, when noises and disturbances occur, the high order un-modeled dynamics could potentially make the conventional controller generates impractical control inputs, while the bioinspired backstepping sliding mode controller will provide more consistent control inputs because its a dynamic model.

The overall bioinspired neural dynamic based backstepping sliding mode control law is proposed in (32) and (45) to (47), the progressive stability design through the backstepping design technique ensures the stability of the proposed control.

3.4. Adaptive sliding innovation filter

The quadrotor UAV often operates in complicated noisy environments, therefore, having accurate state estimates is crucial to ensure the tracking performance. In addition, since the quadrotor operates under disturbances, the accurate system model cannot be obtained. To address this issue, the newly proposed ASIF is integrated with the control design, this filter is robust against modeling errors [37]. The basic design of the ASIF is similar to the sliding mode state observer and Kalman filter; it first goes through a predicting stage, which is illustrated in three main functions as

$$P_{k+1|k} = \bar{A}P_{k|k} + \bar{B}u_k \tag{49}$$

$$\bar{E}_{k+1|k} = \bar{A}\bar{E}_{k|k}\bar{A}^T + Q_{k+1} \tag{50}$$

$$z_{k+1|k} = \tilde{P}_{k+1} - \bar{C}\hat{P}_{k+1|k} \tag{51}$$

where $\hat{P}_{k|k}$ and $\hat{P}_{k+1|k}$ are respectively the posterior and priori state estimates at time step k; $\tilde{P}_{k+1}$ is the measured states, and $P = [\eta_x, \dot{\eta}_x, \dots, \xi_\psi, \dot{\xi}_\psi]^T$; $\bar{E}_{k+1|k}$ is the state error covariance; $\bar{C}$ is the measurement matrix; $z_{t+1|t}$ is the innovation. The system matrix $\bar{A}$ that is used to estimate the state is an identity matrix, which is given as I_{12}; $\bar{B}$ is defined as time step Δt and u_k is the input.

After that, these predicted variables are processed through the update stage as

$$K_{k+1} = C^+\mathrm{diag}(\mathrm{sat}\left(\frac{|\hat{P}_{k+1|k}|}{\rho}\right)) \tag{52}$$

$$\hat{P}_{k+1|k+1} = \hat{P}_{k+1|k} + K_{k+1}\hat{P}_{k+1|k} \tag{53}$$

$$\begin{aligned}\bar{E}_{k+1|k+1} =& (I - K_{k+1}C)E_{k+1|k}(I - K_{k+1}C)^T \\ &+ K_{k+1}R_{k+1}K_{k+1}{}^T\end{aligned} \tag{54}$$

where ρ is the sliding boundary that is manually tuned in the conventional design and C^+ is the pseudoinverse of the measurement matrix.

The design of the conventional sliding innovation filter has been completed, it is noted that the conventional design does not consider the system noise covariance, thus it only provides suboptimal results. To improve the accuracy of the state estimates, the sliding boundary and sliding innovation gain are replaced by

$$S_{k+1} = CE_{k+1|k}C^T + R_{k+1} \tag{55}$$

$$\rho_{k+1} = S_{k+1}(S_{k+1} - R_{k+1})^{-1}\mathrm{diag}|\hat{z}_{k+1|k}| \tag{56}$$

$$K_{k+1} = C^+\mathrm{diag}|\hat{z}_{k+1|k}|\rho_{k+1}^{-1} \tag{57}$$

where W_{k+1} is the innovation covariance. Thus, the overall design of the ASIF for the quadrotor is presented. It is worth mentioning that the design of the controller is based on the state estimates from ASIF and its stability has been guaranteed in [38]. The tracking error is obtained using the desired state and estimated state, under this circumstance, the stability of the proposed control method can be guaranteed by treating the estimation error as part of the disturbances.

Table 1
Quadrotor UAV parameters.

Parameter	Value	Parameter	Value
m (kg)	0.486	g (m/s^2)	9.810
I_r (kg·m^2)	2.830e^{-5}	d (m)	0.250
k_p (N·s^2)	3.230e^{-7}	d (N·m·s^2)	2.980e^{-5}
I_{xx}, I_{yy} (kg·m^2)	4.856e^{-3}	I_{zz} (kg·m^2)	8.801e^{-3}
c_{dx}, c_{dy} (kg/s)	5.560e^{-4}	c_{dz} (kg/s)	6.350e^{-4}

Table 2
Control parameters.

Parameter	Value	Parameter	Value
$A_{1x,y,z}$	1, 1, 1	$A_{2x,y,z}$	4, 4, 4
$A_{3\phi,\theta,\psi}$	5, 5, 5	$A_{4\phi,\theta,\psi}$	2, 2, 2
$B_{1x,y,z}$	2, 2, 2	$B_{2x,y,z}$	8, 8, 8
$B_{3\phi,\theta,\psi}$	1, 1, 1	$B_{4\phi,\theta,\psi}$	10, 10, 10
$D_{1x,y,z}$	2, 2, 2	$D_{2x,y,z}$	8, 8, 8
$D_{3\phi,\theta,\psi}$	1, 1, 1	$D_{4\phi,\theta,\psi}$	10, 10, 10
$K_{1x,y,z}$	0.1, 0.1, 0.1	$K_{2x,y,z}$	1, 1, 1
$K_{3\phi,\theta,\psi}$	3, 3, 3	$K_{4\phi,\theta,\psi}$	5, 5, 5

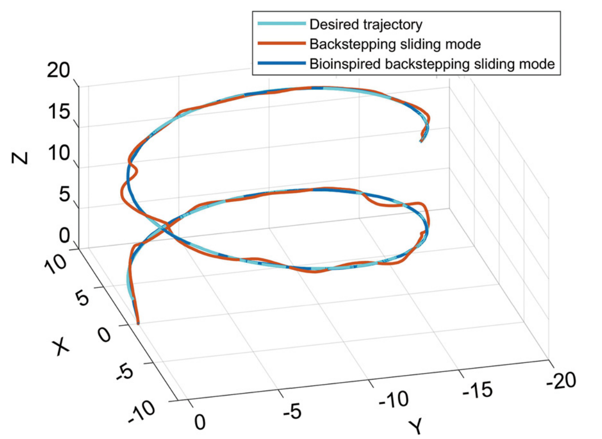

Fig. 3. The quadrotor position estimates in 3D space.

4. Results

This section shows the results that demonstrate the efficiency and effectiveness of the proposed bioinspired control strategy that is integrated with the ASIF. The sampling time Δt is set to be 0.01 s. The quadrotor UAV parameters and control parameters for the bioinspired backstepping sliding mode control are respectively shown in Tables 1 and 2 with the initial conditions set to be zeros for all states. As for the backstepping sliding mode control, the control parameters are the same as shown in Table 2 with the sign function in the conventional method being replaced by the saturation function, the limits of the saturation function are accordingly set to be the same as the upper bound and the lower bound of the shunting model as B_i and $-D_i$. As for the tuning of the control parameters, it is obvious there are many control parameters, one main aspect is that the rotational control parameters need to be higher than the translational control parameters because if the translational dynamics converges fast would result in a large steady state tracking error because the rotational dynamics never converges. The desired path is defined as $x_d = 1 + 8\sin(0.1t)$, $y_d = -8 + 8\cos(0.1t)$, $z_d = 2 + 0.2t$, and $\psi_d = 0.2$. The proposed control method is then used to track this path under noises and disturbances.

4.1. Control performance under noises

In real world applications, the quadrotor usually works under hard conditions, in which system and measurement noises take critical roles in tracking performance. Therefore, the proposed control is used to track a helix path, the initial position of the quadrotor UAV is set to $(0, 0, 0)$ and $\psi_a = 0$. The system and measurement noises are both treated as Gaussian distributed, and the covariances of the system and the noise of measurement Q, R are both treated as diag10^{-6}[0.1, 1, 0.01, 0.1, 0.01, 0.1, 1, 10, 1, 10, 1, 10].

As seen in Figs. 3 and 4, although both conventional and bioinspired control methods are capable of tracking the desired path. However, it can be seen the tracking performance of the proposed bioinspired control strategy has apparent advantages, the steady state tracking error has been sufficiently reduced under the noises. In addition, the shunting model has filtering capability, which means the control inputs are smooth. As seen in Fig. 5, the control input for conventional backstepping control suffers from large chattering issue, especially for U_2 and U_3, this is due to the fact that the desired states that are calculated through the output of translational controller in (31), which suffers from the effects of the noises. This control smoothness makes the proposed control a more practical solution for quadrotor UAV operating under noises in real world applications.

Remark 5. The filtering capability of the bioinspired method is capable of providing smooth control inputs, this means in order to track a desired path, the bioinspired backstepping sliding mode control that requires less control effort compare to conventional methods. In addition, these control inputs would be converted to the rotational speed of rotors through (14), this means the large discontinuities in U_2 and U_3 make the rotor impossible to reach such fast changing rotational speed demand under noises, however, the bioinspired backstepping sliding mode control has efficiently solved the such issue and ensured the smooth transition of the rotors rotational speeds.

4.2. Control performance under disturbances

Since the quadrotor UAV usually operates in outdoor environments, the disturbances such as wind is an unavoidable problem that quadrotor UAV has to face. Therefore, this subsection tests the performance of the proposed bioinspired control method under disturbances. The disturbances are defined as $d_\phi = d_\theta = 0.4$, $d_\psi = 0.4\sin(t)$, $d_x = d_y = 0.1\sin(t)$, and $d_z = 0.1\cos(t)$. The results are shown in Fig. 6. It is undoubtedly that the proposed bioinspired control strategy is more robust than the conventional method, in addition, since there are more parameters that can be tuned, better results can be achieved.

Remark 6. In order to reduce the effects of disturbances, the conventional method usually requires high gain control to counter these effects. However, due to the state constraints of the backstepping control design, ϕ and θ have to stay between $(-\pi/2, \pi/2)$. This high gain control in conventional design would make the quadrotor impossible to achieve and reach quadrotor state constraints. The proposed bioinspired method is capable of providing a relatively smoother control command transition, thus reducing the possibility for a quadrotor UAV reaching its state constraint.

Remark 7. It is noted that if large initial tracking errors occur, the conventional design will yield large initial control inputs; however, this issue is avoided in the bioinspired control design, since the output of the shunting model is strictly bounded between the finite interval $(-D_i, B_i)$, thus preventing a higher control input at the initial stage. Again, this is quite important in quadrotor backstepping based control design because a larger initial control input would make quadrotor UAV reach its state constraints, thus impossible for actuator to reach.

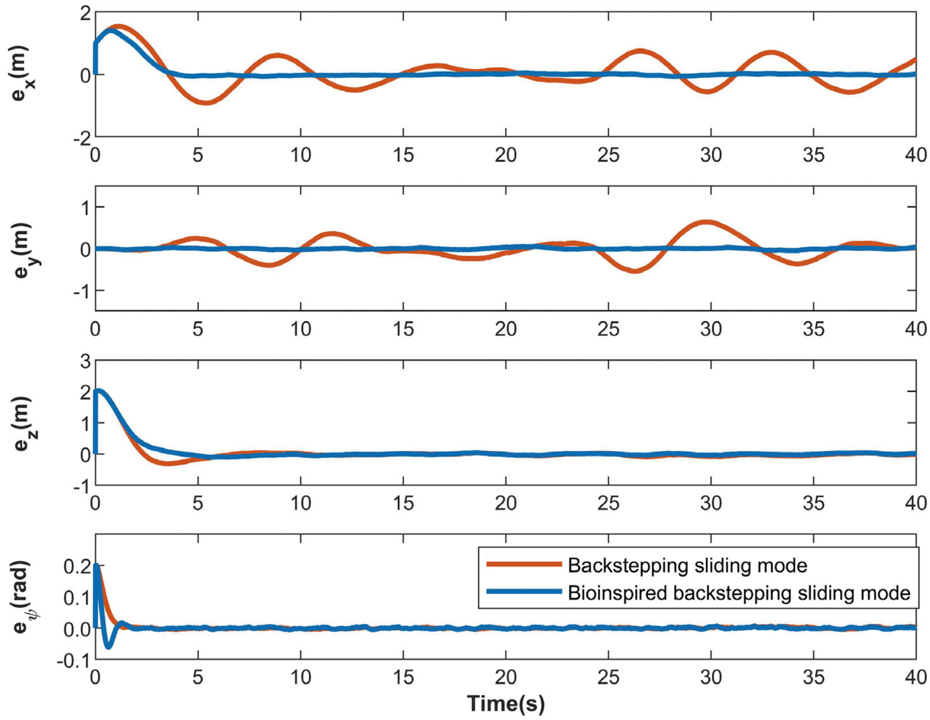

Fig. 4. Tracking error under noises.

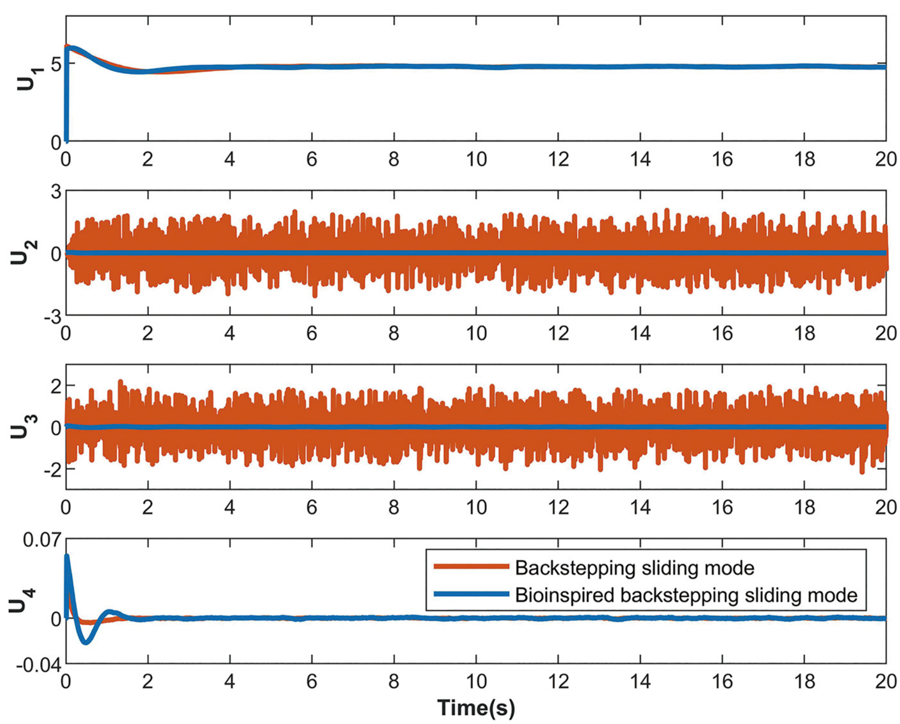

Fig. 5. Control inputs under noises.

4.3. State estimates under noises and faulty conditions

The robustness of providing accurate state estimates is another important aspect to ensure that a quadrotor works properly. Some commonly known filters, such as the Kalman filter (KF) or extended Kalman filter (EKF), these filters provide accurate state estimates only based on the assumption that the modeling of the system is fully known. Therefore, this paper developed a bioinspired control and ASIF to provide accurate state estimates under modeling errors. Since there exist disturbances, therefore, the accurate system model cannot be obtained, in addition, the quadrotor UAV often operates in complex environments, thus, the estimator could fail if the UAV is not well maintained or under electromagnetic inferences. The root mean square error (RMSE) is used to demonstrate the differences between the estimated states and the actual states. Under normal working conditions without

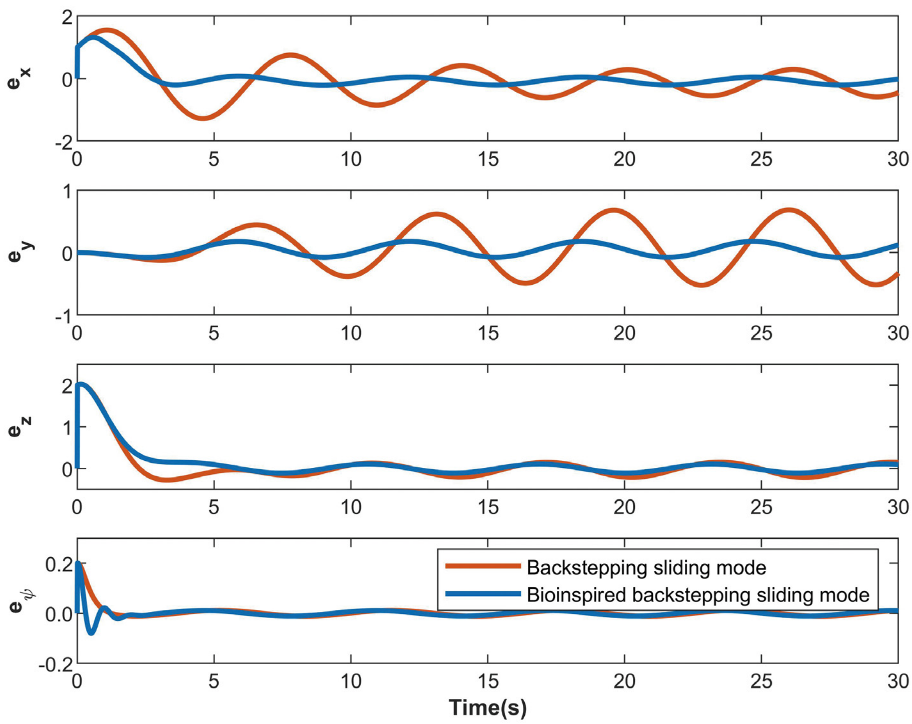

Fig. 6. Tracking error under disturbances.

Table 3
RMSE under normal conditions (Multiply by 10^{-4}).

States	ASIF	KF	States	ASIF	KF
η_x	7.88	7.88	$\dot{\eta}_x$	24.8	24.8
η_y	7.75	7.75	$\dot{\eta}_y$	25.0	25.0
η_z	7.80	7.80	$\dot{\eta}_z$	24.5	24.5
ξ_ψ	2.52	2.52	$\dot{\xi}_\psi$	7.56	7.56
ξ_ϕ	2.47	2.47	$\dot{\xi}_\phi$	7.77	7.77
ξ_θ	2.47	2.47	$\dot{\xi}_\theta$	7.66	7.66

Table 4
RMSE under disturbances (Multiply by 10^{-4}).

States	ASIF	KF	States	ASIF	KF
η_x	7.87	7.89	$\dot{\eta}_x$	39.3	61.8
η_y	7.82	7.83	$\dot{\eta}_y$	39.2	53.4
η_z	7.84	7.85	$\dot{\eta}_z$	37.8	42.1
ξ_ψ	2.49	2.50	$\dot{\xi}_\psi$	15.7	35.9
ξ_ϕ	2.49	2.50	$\dot{\xi}_\phi$	15.1	50.0
ξ_θ	2.47	2.50	$\dot{\xi}_\theta$	15.1	47.2

noises and disturbances. As seen in Table 3, it is noticed that the ASIF provides identical state estimates as the Kalman filter does.

However, when the system operates under large disturbances, such disturbances has been enlarged by four times. Then, Table 4 clearly indicates that the ASIF has successfully provided better state estimates than the KF under both disturbances and noises. It is worth mentioning that when modeling errors occur in the filter, such as the mass being wrongly calculated, the ASIF is still capable of providing more accurate state estimates than KF. It is discovered that under large disturbances or modeling uncertainties, the filtering would weight to trust measurement instead of prediction, thus providing better state estimates.

5. Conclusion

In this paper, the bioinspired based backstepping sliding mode control for quadrotor UAV is proposed, which is then integrated with the ASIF. The proposed control strategy is robust to disturbances; meanwhile, under system and measurement noises, the proposed control is capable of providing relatively smooth control input with better tracking performances. Thus, this controller has successfully addressed both noises and disturbances issues with the aid of the bioinspired neural dynamics with proof of the stability. In addition, considering the modeling error from the disturbances, the ASIF is integrated with the proposed bioinspired control to provide more accurate state estimates under disturbances to achieve better control performance.

In future works, the tuning of the control parameters could be further addressed using optimization techniques and the state constraints could be considered to improve the tracking performance of the proposed control.

Declaration of competing interest

The authors declare that they have no known competing financial interests or personal relationships that could have appeared to influence the work reported in this paper.

Acknowledgement

This work was supported by the Natural Sciences and Engineering Research Council (NSERC) of Canada.

References

[1] M. Tao, Q. Chen, X. He, S. Xie, Fixed-time filtered adaptive parameter estimation and attitude control for quadrotor UAVs, IEEE Trans. Aerosp. Electron. Syst. 58 (5) (2022) 4135–4146, http://dx.doi.org/10.1109/TAES.2022.3159770.

[2] M. Zhao, Y. Zou, Q. Fu, W. He, Effects of airfoil on aerodynamic performance of flapping wing, Biomim. Intell. Robotics 1 (May) (2021) 100004, http://dx.doi.org/10.1016/j.birob.2021.100004.

[3] S. Liang, B. Song, D. Xue, Landing route planning method for micro drones based on hybrid optimization algorithm, Biomim. Intell. Robotics 1 (May) (2021) 100003, http://dx.doi.org/10.1016/j.birob.2021.100003.

[4] J. Chen, C. Luo, M. Krishnan, M. Paulik, Y. Tang, An enhanced dynamic delaunay triangulation-based path planning algorithm for autonomous mobile robot navigation, in: Intelligent Robots and Computer Vision XXVII: Algorithms and Techniques, Vol. 7539, SPIE, 2010, p. 75390P, http://dx.doi.org/10.1117/12.838966.

[5] T. Yan, Z. Xu, S.X. Yang, Consensus formation control for multiple AUV systems using distributed bioinspired sliding mode control, IEEE Trans. Intell. Veh. 8 (2) (2022) 1081–1092, http://dx.doi.org/10.1109/TIV.2022.3175647.

[6] L. Liu, Luo Chaomin, F. Shen, Multi-agent formation control with target tracking and navigation, in: IEEE International Conference on Information and Automation, ICIA, Macau, China, 2017, pp. 98–103, http://dx.doi.org/10.1109/ICInfA.2017.8078889.

[7] Z. Chu, X. Xiang, D. Zhu, C. Luo, D. Xie, Adaptive trajectory tracking control for remotely operated vehicles considering thruster dynamics and saturation constraints, ISA Trans. 100 (2020) 28–37, http://dx.doi.org/10.1016/j.isatra.2019.11.032.

[8] B. Li, W. Gong, Y. Yang, B. Xiao, D. Ran, Appointed fixed time observer-based sliding mode control for a quadrotor UAV under external disturbances, IEEE Trans. Aerosp. Electron. Syst. 58 (1) (2022) 290–303, http://dx.doi.org/10.1109/TAES.2021.3101562.

[9] M. Labbadi, M. Cherkaoui, Robust adaptive backstepping fast terminal sliding mode controller for uncertain quadrotor UAV, Aerosp. Sci. Technol. 93 (2019) 105306, http://dx.doi.org/10.1016/j.ast.2019.105306.

[10] B. Zhao, Y. Tang, C. Wu, W. Du, Vision-based tracking control of quadrotor with backstepping sliding mode control, IEEE Access 6 (2018) 72439–72448, http://dx.doi.org/10.1109/ACCESS.2018.2882241.

[11] M. Labbadi, A.J. Muñoz-Vázquez, M. Djemai, Y. Boukal, M. Zerrougui, M. Cherkaoui, Fractional-order nonsingular terminal sliding mode controller for a quadrotor with disturbances, Appl. Math. Model. 111 (2022) 753–776, http://dx.doi.org/10.1016/j.apm.2022.07.016.

[12] J. Wang, K.A. Alattas, Y. Bouteraa, O. Mofid, S. Mobayen, Adaptive finite-time backstepping control tracker for quadrotor UAV with model uncertainty and external disturbance, Aerosp. Sci. Technol. 133 (2023) 108088, http://dx.doi.org/10.1016/j.ast.2022.108088.

[13] B. Gao, Y.J. Liu, L. Liu, Adaptive neural fault-tolerant control of a quadrotor UAV via fast terminal sliding mode, Aerosp. Sci. Technol. 129 (2022) 107818, http://dx.doi.org/10.1016/j.ast.2022.107818.

[14] D. Lam, C. Manzie, M.C. Good, Model predictive contouring control for biaxial systems, IEEE Trans. Control Syst. Technol. 21 (2) (2013) 552–559, http://dx.doi.org/10.1109/TCST.2012.2186299.

[15] L. Xi, X. Wang, L. Jiao, S. Lai, Z. Peng, B.M. Chen, GTO-MPC-Based target chasing using a quadrotor in cluttered environments, IEEE Trans. Ind. Electron. 69 (6) (2022) 6026–6035, http://dx.doi.org/10.1109/TIE.2021.3090700.

[16] I. Lopez-Sanchez, F. Rossomando, R. Pérez-Alcocer, C. Soria, R. Carelli, J. Moreno-Valenzuela, Adaptive trajectory tracking control for quadrotors with disturbances by using generalized regression neural networks, Neurocomputing 460 (2021) 243–255, http://dx.doi.org/10.1016/j.neucom.2021.06.079.

[17] H. Razmi, S. Afshinfar, Neural network-based adaptive sliding mode control design for position and attitude control of a quadrotor UAV, Aerosp. Sci. Technol. 91 (2019) 12–27, http://dx.doi.org/10.1016/j.ast.2019.04.055.

[18] H. Liu, B. Li, B. Xiao, D. Ran, C. Zhang, Reinforcement learning-based tracking control for a quadrotor unmanned aerial vehicle under external disturbances, Internat. J. Robust Nonlinear Control 2022 (2022) 1–18, http://dx.doi.org/10.1002/rnc.6334.

[19] M. Li, Z. Cai, J. Zhao, J. Wang, Y. Wang, Disturbance rejection and high dynamic quadrotor control based on reinforcement learning and supervised learning, Neural Comput. Appl. 34 (13) (2022) 11141–11161, http://dx.doi.org/10.1007/s00521-022-07033-7.

[20] Z. Chu, B. Sun, D. Zhu, M. Zhang, C. Luo, Motion control of unmanned underwater vehicles via deep imitation reinforcement learning algorithm, IET Intell. Transp. Syst. 14 (7) (2020) 764–774, http://dx.doi.org/10.1049/iet-its.2019.0273.

[21] M. Chen, S. Xiong, Q. Wu, Tracking flight control of quadrotor based on disturbance observer, IEEE Trans. Syst. Man Cybern. 51 (3) (2021) 1414–1423, http://dx.doi.org/10.1109/TSMC.2019.2896891.

[22] F. Wang, H. Gao, K. Wang, C. Zhou, Q. Zong, C. Hua, Disturbance observer-based finite-time control design for a quadrotor UAV with external disturbance, IEEE Trans. Aerosp. Electron. Syst. 57 (2) (2021) 834–847, http://dx.doi.org/10.1109/TAES.2020.3046087.

[23] L. Chen, Z. Liu, Q. Dang, W. Zhao, G. Wang, Robust trajectory tracking control for a quadrotor using recursive sliding mode control and nonlinear extended state observer, Aerosp. Sci. Technol. 128 (2022) 107749, http://dx.doi.org/10.1016/j.ast.2022.107749.

[24] L. Zhou, J. Zhang, J. Dou, B. Wen, A fuzzy adaptive backstepping control based on mass observer for trajectory tracking of a quadrotor UAV, Internat. J. Adapt. Control Signal Process. 32 (12) (2018) 1675–1693, http://dx.doi.org/10.1002/acs.2937.

[25] S. Huang, J. Huang, Z. Cai, H. Cui, Adaptive backstepping sliding mode control for quadrotor UAV, Sci. Program. 2021 (2021) http://dx.doi.org/10.1155/2021/3997648.

[26] J.R. Azinheira, A. Moutinho, Hover control of an UAV with backstepping design including input saturations, IEEE Trans. Control Syst. Technol. 16 (3) (2008) 517–526, http://dx.doi.org/10.1109/TCST.2007.908209.

[27] Q. Xu, Z. Wang, Z. Zhen, Information fusion estimation-based path following control of quadrotor UAVs subjected to Gaussian random disturbance, ISA Trans. 99 (2020) 84–94, http://dx.doi.org/10.1016/j.isatra.2019.10.003.

[28] M. Labbadi, M. Cherkaoui, Adaptive fractional-order nonsingular fast terminal sliding mode based robust tracking control of quadrotor UAV with Gaussian random disturbances and uncertainties, IEEE Trans. Aerosp. Electron. Syst. 57 (4) (2021) 2265–2277, http://dx.doi.org/10.1109/TAES.2021.3053109.

[29] F. Chen, R. Jiang, K. Zhang, B. Jiang, G. Tao, Robust backstepping sliding-mode control and observer-based fault estimation for a quadrotor UAV, IEEE Trans. Ind. Electron. 63 (8) (2016) 5044–5056, http://dx.doi.org/10.1109/TIE.2016.2552151.

[30] A. Hodgkin, Huxley, A quantitative description of membrane current and its application to conduction and excitation in nerve, J. Physiol. 117 (4) (1952) 500–544, http://dx.doi.org/10.1113/jphysiol.1952.sp004764.

[31] S. Grossberg, Nonlinear neural networks : Principles, mechanisms, and architectures, Neural Netw. 1 (1) (1988) 17–61, http://dx.doi.org/10.1016/0893-6080(88)90021-4.

[32] S.X. Yang, M. Meng, An efficient neural network approach to dynamic robot motion planning, Neural Netw. 13 (2) (2000) 143–148, http://dx.doi.org/10.1016/s0893-6080(99)00103-3.

[33] D. Zhu, B. Sun, The bio-inspired model based hybrid sliding-mode tracking control for unmanned underwater vehicles, Eng. Appl. Artif. Intell. 26 (10) (2013) 2260–2269, http://dx.doi.org/10.1016/j.engappai.2013.08.017.

[34] S.X. Yang, A. Zhu, G. Yuan, M.Q. Meng, A bioinspired neurodynamics-based approach to tracking control of mobile robots, IEEE Trans. Ind. Electron. 59 (8) (2012) 3211–3220.

[35] J. Ni, L. Wu, P. Shi, S.X. Yang, A dynamic bioinspired neural network based real-time path planning method for autonomous underwater vehicles, Comput. Intell. Neurosci. 2017 (2017) 1–16, http://dx.doi.org/10.1155/2017/9269742.

[36] D. Zhu, B. Zhou, S.X. Yang, A novel algorithm of multi-AUVs task assignment and path planning based on biologically inspired neural network map, IEEE Trans. Intell. Veh. 6 (2) (2021) 333–342, http://dx.doi.org/10.1109/TIV.2020.3029369.

[37] A.S. Lee, S.A. Gadsden, M. Al-Shabi, An adaptive formulation of the sliding innovation filter, IEEE Signal Process. Lett. 28 (2021) 1295–1299, http://dx.doi.org/10.1109/LSP.2021.3089918.

[38] S. Andrew Gadsden, M. Al-Shabi, The sliding innovation filter, IEEE Access 8 (2020) 96129–96138, http://dx.doi.org/10.1109/ACCESS.2020.2995345.